Dual strands of pre-*miR-150* (*miR-150-5p* and *miR-150-3p*) act as antitumor miRNAs targeting *SPOCK1* in naïve and castration-resistant prostate cancer

ATSUSHI OKATO[1,2], TAKAYUKI ARAI[1,2], SATOKO KOJIMA[3], KEIICHI KOSHIZUKA[1], YUSAKU OSAKO[4], TETSUYA IDICHI[4], AKIRA KUROZUMI[1,2], YUSUKE GOTO[1,2], MAYUKO KATO[1,2], YUKIO NAYA[3], TOMOHIKO ICHIKAWA[2] and NAOHIKO SEKI[1]

Departments of [1]Functional Genomics and [2]Urology, Chiba University Graduate School of Medicine, Chiba; [3]Department of Urology, Teikyo University Chiba Medical Center, Ichihara; [4]Department of Digestive Surgery, Breast and Thyroid Surgery, Graduate School of Medical Sciences, Kagoshima University, Kagoshima, Japan

Received March 7, 2017; Accepted April 21, 2017

DOI: 10.3892/ijo.2017.4008

Abstract. Analysis of our microRNA (miRNA) expression signature in human cancers has shown that guide and passenger strands of pre-*miR-150*, i.e., *miR-150-5p* and *miR-150-3p*, are significantly downregulated in cancer tissues. In miRNA biogenesis, the passenger strand of miRNA is degraded and is thought to have no functions. Thus, the aim of this study was to investigate the functional significance of *miR-150-5p* and *miR-150-3p* in naïve prostate cancer (PCa) and castration-resistant prostate cancer (CRPC). Ectopic expression assays showed that both strands of miRNAs significantly suppressed cancer cell migration and invasion. Our strategies of miRNA target searching demonstrated that *SPOCK1* (*SPARC/osteonectin, cwcv* and *kazal like domains proteoglycan 1*) was directly regulated by *miR-150-5p* and *miR-150-3p*. Knockdown of *SPOCK1* by siRNA inhibited cancer cell aggressiveness. Moreover, overexpression of SPOCK1 was observed in naïve PCa and CRPC tissues. Taken together, dual strands of pre-*miR-150* (*miR-150-5p* and *miR-150-3p*) acted as antitumor miRNAs in naïve PCa and CRPC cells. Expression of oncogenic *SPOCK1* was involved in naïve PCa and CRPC pathogenesis. Novel approaches to analysis of antitumor miRNA-regulated RNA networks in cancer cells may provide new insights into the pathogenic mechanisms of naïve PCa and CRPC.

Introduction

Prostate cancer (PCa) is the most frequently diagnosed cancer among men in developed countries (1). Although PCa is initially responsive to androgen-deprivation therapy (ADT), most patients experience disease relapse and develop castration-resistant prostate cancer (CRPC) (2). The survival rate of patients with CRPC is poor owing to the occurrence of metastasis (3) and patients with metastatic CRPC cannot be effectively treated using recently developed molecular-targeted therapies (2,3). Therefore, new treatment strategies are needed for these patients. The molecular mechanisms underlying the aggressiveness of CRPC cells and the acquisition of treatment resistance are still unclear.

MicroRNAs (miRNAs) are noncoding RNAs that act as sequence-specific fine tuners for regulating the expression levels of proteins and RNAs (4,5). Notably, a single miRNA can regulate a large number of RNA transcripts in human cells (6). Accordingly, dysregulation of miRNAs can disrupt the tightly regulated RNA networks in cancer cells, leading to cancer cell initiation, development, metastasis, and drug resistance (7,8). The discovery of miRNAs has complicated the analysis of intracellular RNA networks in cancer.

We recently constructed an RNA-sequence based miRNA expression signature using autopsy specimens from patients with CRPC (9). To elucidate the miRNA-mediated RNA networks in metastatic CRPC, we have sequentially identified antitumor miRNAs and oncogenic genes regulated by these miRNAs based on our miRNA expression signatures (9,10). Analysis of our miRNA signatures, including that in CRPC, has shown that both strands of pre-*miR-150*, i.e., *miR-150-5p* (the guide strand) and *miR-150-3p* (the passenger strand), are significantly reduced in cancer tissues (9).

In miRNA biogenesis, pre-miRNA is cleaved by Dicer into the miRNA duplex, containing the guide and passenger strands. The mature guide strand miRNA is incorporated into the RNA-induced silencing complex (RISC) and represses mRNA translation or cleaves mRNA (11). In contrast, the passenger strand of miRNA was previously thought to be degraded and to have no function (12-14). However, our expression data have contradicted this established miRNA theory. We hypothesized that the passenger strand of *miR-150-3p* may have functions in naïve PCa and CRPC cells by targeting novel oncogenic

Correspondence to: Dr Naohiko Seki, Department of Functional Genomics, Chiba University Graduate School of Medicine, 1-8-1 Inohana, Chuo-ku, Chiba 260-8670, Japan
E-mail: naoseki@faculty.chiba-u.jp

Key words: microRNA, *miR-150-5p*, *miR-150-3p*, prostate cancer, castration-resistant prostate cancer, *SPOCK*

Table I. Characteristics of patients with non-PCa and naïve PCa and CRPC.

No.	Diagnosis	Age (years)	PSA (ng/ml)	Gleason score	T	N	M	Stage
1	Non-PCa	57	5.71	-	-	-	-	-
2	Non-PCa	74	9.45	-	-	-	-	-
3	Non-PCa	70	8.58	-	-	-	-	-
4	Non-PCa	73	4.8	-	-	-	-	-
5	Non-PCa	67	6.91	-	-	-	-	-
6	Non-PCa	50	7.05	-	-	-	-	-
7	Non-PCa	74	9.91	-	-	-	-	-
8	Non-PCa	76	20.9	-	-	-	-	-
9	Non-PCa	59	4.5	-	-	-	-	-
10	Non-PCa	75	1.1	-	-	-	-	-
11	Non-PCa	60	7.29	-	-	-	-	-
12	Non-PCa	73	38.7	-	-	-	-	-
13	Non-PCa	69	11.9	-	-	-	-	-
14	Non-PCa	77	23.3	-	-	-	-	-
15	Non-PCa	61	4.57	-	-	-	-	-
16	Non-PCa	59	7.37	-	-	-	-	-
17	Non-PCa	65	5.06	-	-	-	-	-
18	PCa	70	75.7	4+5	4	1	1	D2
19	PCa	78	1,800	4+5	4	1	1	D2
20	PCa	75	68.4	5+4	4	1	0	D1
21	PCa	62	38.7	4+5	2b	1	0	D1
22	PCa	70	25.5	4+5	3b	0	0	C
23	PCa	75	1,260	4+5	3b	1	1	D2
24	PCa	88	888	4+5	3b	1	1	D2
25	PCa	69	33.9	4+5	4	0	1	D2
26	PCa	62	62.3	4+5	3b	1	0	D1
27	PCa	78	5	4+5	2c	0	1b	D2
28	PCa	64	449	4+5	3b	1	1	D2
29	PCa	81	365	4+5	4	1	1	D2
30	PCa	76	715	5+4	4	1	1	D2
31	PCa	79	555	4+5	3	1	1	D2
32	PCa	63	1,120	4+5	2c	0	1b	D2
33	PCa	67	4.95	4+5	4	1	1b	D2
34	PCa	70	19.5	5+5	4	1	1c	D2
35	CRPC	69	15.8	5+4	3b	1	1	D2
36	CRPC	72	212	5+4	4	1	1	D2
37	CRPC	71	4.4	4+5	4	1	1	D2
38	CRPC	66	295	4+5	4	1	1	D2
39	CRPC	68	7.54	4+5	4	1	1b	D2

genes. Accordingly, in this study, we aimed to investigate the functional significance of *miR-150-5p* and *miR-150-3p* in naïve PCa and CRPC cells and to identify oncogenic genes involved in the pathogenesis of the disease.

Materials and methods

Clinical prostate specimens. Clinical prostate specimens were obtained from patients admitted to Teikyo University Chiba Medical Center from 2014 to 2015. All patients had elevated prostate-specific antigen (PSA) and had undergone transrectal biopsies for definitive cancer diagnoses. Particularly, in patients with CRPC, neuroendocrine differentiation was excluded. The patient backgrounds are summarized in Table I. Samples were staged according to the UICC TNM classification (15).

All patients in this study provided written informed consent for tissue donation for research purposes. The protocol

was approved by the Institutional Review Boards of Chiba University and Teikyo University.

Tissue collection and cell culture. Prostate tissues were immersed in RNAlater (Thermo Fisher Scientific, Waltham, MA, USA) and stored at 4˚C until RNA extraction. Human prostate cancer cells (PC3 and PC3M cells) were obtained from the American Type Culture Collection (Manassas, VA, USA).

Quantitative real-time reverse transcription polymerase chain reaction (RT-q-PCR). Stem-loop RT-PCR (TaqMan MicroRNA assays; product ID: 000473 for *miR-150-5p* and 002637 for *miR-150-3p*; Applied Biosystems, Foster City, CA, USA) was used in this assays. TaqMan probes and primers for *SPOCK1* (product ID: Hs00270274_m1; Applied Biosystems) were assay-on-demand gene expression products. We used *GUSB* (product ID: Hs00939627_m1; Applied Biosystems), *GAPDH* (product ID: Hs02758991_g1; Applied Biosystems), and *RNU48* (product ID: 001006; Applied Biosystems) as internal controls.

Cell proliferation, migration, and invasion assays. Cell proliferation, migration, and invasion assays were carried out as previously described (9,10).

Argonaute 2 (AGO2)-bound miRNA isolation by immunoprecipitation. PC3 cells were transfected with 10 nM miRNA by reverse transfection and plated in 10-cm plates at $1x10^5$ cells/ml. After 48 h, immunoprecipitation was performed using a microRNA Isolation kit, Human Ago2 (Wako, Osaka, Japan) according to the manufacturer's protocol. Expression levels of miRNAs bound to Ago2 were measured by TaqMan RT-qPCR. miRNA expression data were normalized to the expression of *miR-26a* (product ID: 000404; Applied Biosystems), which was not affected by *miR-150-5p* and *miR-150-3p*.

Western blot analysis. Immunoblotting was conducted with diluted monoclonal anti-SPOCK1 antibodies (1:100 dilution; sc-398782; Santa Cruz Biotechnology, Santa Cruz, CA, USA) and with diluted anti-glyceraldehyde 3-phosphate dehydrogenase (GAPDH) antibodies (1:1,000 dilution; ab8245; Abcam, Cambridge, UK) as a loading control. The procedures were performed as previously described (16).

Selection of putative target genes regulated by miR-150-5p and miR-150-3p in PCa cells. To identify *miR-150-5p* and *miR-150-3p* target genes, we analyzed gene expression profile (Gene Expression Omnibus database; accession no. GSE29079). Gene expression data were obtained from *miR-150-5p* and *miR-150-3p* transfectant PC3 cells (A SurePrint G3 Human 60K, Agilent Technologies, Santa Clara, CA, USA). We merged these datasets and selected putative *miR-150-5p* and *miR-150-3p* target genes using the TargetScan database (Release 7.1; http://www.targetscan.org/vert_71/).

Plasmid construction and dual-luciferase assays. The partial wide-type sequences of the 3'-untranslated region (UTR) of *SPOCK1* or those with a deleted *miR-150-5p* or *miR-150-3p* target site were inserted in the psiCHECK-2 vector (C8021; Promega, Madison, WI, USA). Alternatively, we used sequences that were missing the *miR-150-5p* target site (position 182-188) or *miR-150-3p* target sites (position 1477-1483, position 1749-1756, or position 2593-2599). The procedure for dual-luciferase reporter assays was described previously (17).

Immunohistochemistry using tissue microarrays. We used a tissue microarray of prostate cancer samples obtained from Provitro (Berlin, Germany; cat. no. 401-2209, Lot no. 146.1P), which contained a total of 78 prostate samples (PCa specimens: n=58, prostatic intraepithelial neoplasia: n=10, and normal prostate samples: n=10). Detailed information on these samples is summarized in Table II. The tissue microarray was immunostained following the manufacturer's protocol, as described previously (10,18).

Statistical analysis. The relationships between 2 groups and expression values obtained by RT-PCR were analyzed using Mann-Whitney U tests. The correlations between *miR-150-5p* and *miR-150-3p* expression were evaluated using Spearman's rank test. The relationships among more than 3 variables and numerical values were analyzed using Bonferroni-adjusted Mann-Whitney U tests. We used Expert StatView software (version 5.0 SAS Institute Inc., Cary, NC, USA) for these analyses.

Results

The expression levels of miR-150-5p and miR-150-3p in naïve PCa and CRPC specimens and cell lines. We evaluated the expression levels of *miR-150-5p* and *miR-150-3p* in PCa tissues (PCa: n=17, CRPC: n=5), normal tissues (non-PCa: n=17), and PCa cell lines (PC3 and PC3M cells). The patient backgrounds are summarized in Table I. The expression levels of *miR-150-5p* and *miR-150-3p* were significantly lower in PCa and CRPC tissues than normal tissues (*miR-150-5p*: P=0.0266 and P=0.018, respectively; *miR-150-3p*: P=0.0025 and P=0.0002, respectively; Fig. 1A). There was a positive correlation between expression levels of *miR-150-5p* and *miR-150-3p* (r=0.854, P<0.0001; Fig. 1B).

Effects of ectopic expression of miR-150-5p and miR-150-3p on cell proliferation, migration, and invasion assays in PCa cell lines. To examine the functional roles of *miR-150-5p* and *miR-150-3p*, we performed gain-of-function studies by using PC3 and PC3M cells transfected with mature miRNAs.

XTT assays revealed that proliferation was significantly inhibited in PC3 and PC3M cells transfected with *miR-150-5p* and *miR-150-3p* in comparison with that of mock or miR-control-transfected cells (P<0.0001; Fig. 1C). Wound-healing and Matrigel invasion assays demonstrated significant inhibition of cell migration and invasion in both *miR-150-5p* and *miR-150-3p* transfectants (P<0.0001; Fig. 1D and E).

Both miR-150-5p and miR-150-3p bound to Ago2. We hypothesized that both *miR-150-5p* and *miR-150-3p* may be incorporated into and function as part of the RISC. To test this hypothesis,

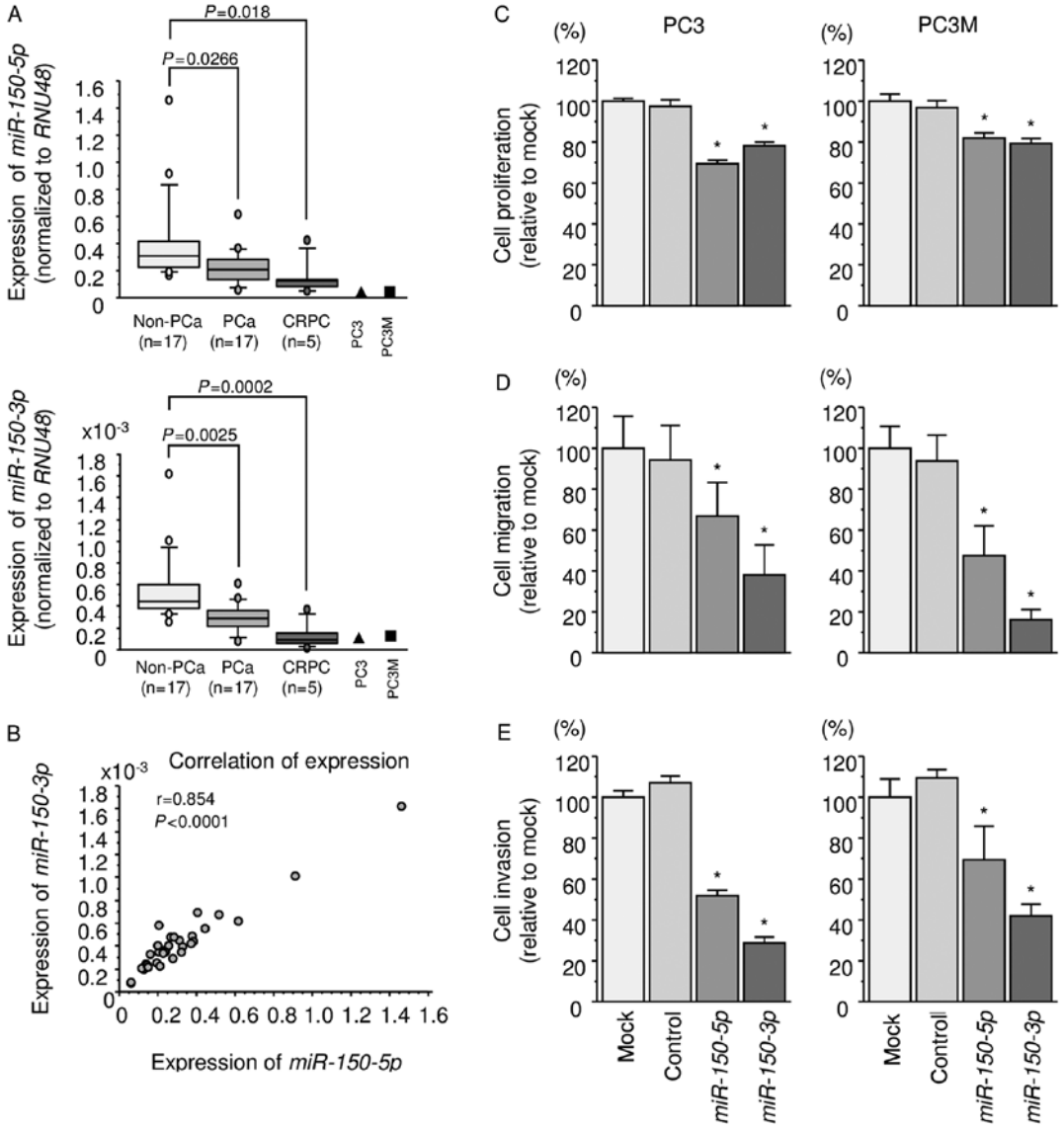

Figure 1. Expression levels of *miR-150-5p* and *miR-150-3p* and functional assays in PCa cell lines (PC3 and PC3M cells) following *miR-150-5p* and *miR-150-3p* transfection. (A) Expression levels of *miR-150-5p* and *miR-150-3p* in naïve PCa and CRPC clinical specimens and cell lines were determined by qRT-PCR. Data were normalized to *RNU48* expression. (B) Correlation between expression levels of *miR-150-5p* and *miR-150-3p*. (r=0.854, P<0.0001). (C) Cell proliferation was determined by XTT assays 72 h after transfection with 10 nM *miR-150-5p* and *miR-150-3p*. *P<0.0001. (D) Cell migration activity was determined by migration assays. *P<0.0001. (E) Cell invasion activity was determined using Matrigel invasion assays. *P<0.0001.

we performed immunoprecipitation with antibodies targeting Ago2, which plays a central role in the RISC. After transfection with *miR-150-5p* or *miR-150-3p*, Ago2-bound miRNAs were isolated, and RT-qPCR was carried out to determine whether *miR-150-5p* and *miR-150-3p* bound to Ago2 (Fig. 2A).

After transfection with *miR-150-5p* and immunoprecipitation by anti-Ago2 antibodies, *miR-150-5p* levels were significantly higher than those of mock- or miR control-transfected cells and those of *miR-150-3p*-transfected PC3 cells (P<0.0001; Fig. 2B). Similarly, after transfection with *miR-150-3p* and immunoprecipitation by anti-Ago2 antibodies, *miR-150-3p* levels were significantly higher than those of mock- or miR control-transfected cells and those of *miR-150-5p*-transfected PC3 cells (P<0.0001; Fig. 2B).

Screening of target genes regulated by miR-150-3p in PCa cells. To obtain further insights into the molecular mechanisms regulated by antitumor *miR-150-3p* in PCa cells, we screened these miRNA-regulated genes by using *in silico* and genome-wide gene expression analyses. First, we undertook genome-wide gene expression analysis using PC3 cells.

Analysis of the TargetScan database showed that 2,558 genes had putative target sites for *miR-150-3p* in their 3'-UTRs. Next, we screened 328 of these genes using genome-wide gene expression analysis. Finally, we found 14 genes that were upregulated (fold-change $\log_2$ >0.5) in cancer tissues by GEO database analyses (GEO accession no. GSE29079). Our strategy for analysis is shown in Fig. 3. Putative target genes of *miR-150-3p* are summarized in Table III. Among these candidate genes, *SPOCK1* had a putative binding site for *miR-150-5p* according to the TargetScan database. Therefore, we focused on *SPOCK1* as a candidate target gene of the dual strands of pre-miR-150 and performed further investigations of this target in PCa.

Table II. Characteristics of patients, as evaluated using immunohistochemistry.

No.	Diagnosis	Age (years)	Gleason score	T	N	IHC score of SPOCK1
1	PCa	64	4+3	3b	0	5
2	PCa	67	3+4	2b	0	3
3	PCa	58	3+4	2b	0	5
4	PCa	63	7	3b	0	6
5	PCa	65	3+3	2b	0	5
6	PCa	61	4+4	3b	×	4
7	PCa	62	3+4	2b	×	2
8	PCa	66	4+4	2b	×	4
9	PCa	61	3+4	3a	×	4
10	PCa	74	4+3	2b	×	5
11	PCa	59	2+3	2b	×	4
12	PCa	69	3+4	3a	0	4
13	PCa	54	3+4	2c	×	6
14	PCa	68	3+4	3a	0	5
15	PCa	58	3+4	3a	0	5
16	PCa	67	3+4	3a	0	4
17	PCa	65	3+3	2a	0	4
18	PCa	77	3+4	4	0	5
19	PCa	64	4+3	2b	0	4
20	PCa	58	3+4	3a	0	6
21	PCa	50	4+3	2b	0	6
22	PCa	53	3+3	2b	0	3
23	PCa	59	4+5	3a	0	5
24	PCa	70	2+3	2b	0	5
25	PCa	65	5+4	3a	0	4
26	PCa	57	3+5	2b	0	5
27	PCa	68	4+4	2b	0	6
28	PCa	58	3+3	2b	0	5
29	PCa	66	3+3	2b	0	3
30	PCa	63	3+4	2b	0	6
31	PCa	56	3+4	2b	0	4
32	PCa	63	5+3	3a	0	3
33	PCa	64	3+5	3a	0	5
34	PCa	60	3+4	2b	0	5
35	PCa	60	3+3	3a	0	5
36	PCa	57	3+2	2b	0	4
37	PCa	50	3+3	2a	0	6
38	PCa	68	3+3	3a	0	5
39	PCa	65	3+4	3b	1	4
40	PCa	69	5+5	3a	1	5
41	PCa	63	3+4	2b	0	5
42	PCa	51	2+3	2b	0	4
43	PCa	62	3+3	3a	0	5
44	PCa	61	3+4	3a	0	5
45	PCa	53	4+4	3b	1	4
46	PCa	56	4+3	2b	0	5
47	PCa	59	2+3	2b	0	5
48	PCa	61	3+4	2b	0	5
49	PCa	51	3+4	3a	0	6

Table II. Continued.

No.	Diagnosis	Age (years)	Gleason score	T	N	IHC score of SPOCK1
50	PCa	62	3+4	3b	1	5
51	PCa	66	3+3	3a	0	5
52	PCa	62	3+3	2b	0	4
53	PCa	56	3+3	2b	0	5
54	PCa	58	3+3	3a	0	5
55	PCa	66	5+4	3a	0	6
56	PCa	55	3+4	3a	0	5
57	PCa	67	2+3	2b	0	5
58	PCa	61	3+5	2b	0	6
59	PIN	59	-	-	-	3
60	PIN	58	-	-	-	5
61	PIN	62	-	-	-	4
62	PIN	51	-	-	-	6
63	PIN	58	-	-	-	3
64	PIN	68	-	-	-	4
65	PIN	64	-	-	-	5
66	PIN	56	-	-	-	5
67	PIN	61	-	-	-	3
68	PIN	51	-	-	-	5
69	Normal	70	-	-	-	4
70	Normal	63	-	-	-	3
71	Normal	62	-	-	-	4
72	Normal	81	-	-	-	0
73	Normal	67	-	-	-	3
74	Normal	76	-	-	-	4
75	Normal	66	-	-	-	4
76	Normal	69	-	-	-	3
77	Normal	63	-	-	-	5
78	Normal	71	-	-	-	4

PCa, prostate cancer; PIN, prostatic intra-epithelial neoplasia.

Regulation of SPOCK1 expression by miR-150-5p and miR-150-3p in PCa cells. Our studies revealed that *SPOCK1* mRNA was significantly reduced in both *miR-150-5p* and *miR-150-3p* transfectants in comparison with those in mock or miR-control transfectants (P<0.0001 and P<0.0001; Fig. 4A). Expression of SPOCK1 protein was also repressed in these miRNAs transfectants (Fig. 4B).

Target prediction databases indicated that *miR-150-5p* had one putative target site in the 3'-UTR of *SPOCK1* (Fig. 4C). Likewise, *miR-150-3p* had three putative target sites (Fig. 4C). To determine whether *SPOCK1* mRNA contained functional target sites, we performed a dual-luciferase reporter assay.

The TargetScan database identified one putative target site in the 3'-UTR of *SPOCK1* for *miR-150-5p* (position 182-188) and three target sites of *SPOCK1* for *miR-150-3p* (positions 1477-1483, 1749-1756, and 2593-2599). We used vectors encoding a partial wild-type sequence of the 3'-UTR of *SPOCK1* mRNA, including the predicted *miR-150-5p* and *miR-150-3p* target site, or a vector lacking the *miR-150-5p* and *miR-150-3p* target sites. We found that the luminescence intensity was significantly reduced by co-transfection with *miR-150-5p* or *miR-150-3p* and the vector carrying the wild-type 3'-UTR of *SPOCK1* (P<0.05; Fig. 4D).

Effects of silencing SPOCK1 on cell proliferation, migration, and invasion in PCa cells. We evaluated the knockdown efficiency of si-*SPOCK1* transfection in PC3 cells. Our present data showed that si-*SPOCK1* transfection effectively downregulated *SPOCK1* expression in PC3 and PC3M cells (Fig. 5A and B).

Functional assays demonstrated that cell proliferation, migration, and invasion were inhibited in si-*SPOCK1* transfec-

Table III. Putative target genes regulated by *miR-150-3p* in PCa cells.

Entrez gene ID	Gene symbol	Gene name	PC3 *miR-150-3p* transfectant (log_2 ratio)	Site counts	GEO Fold change
55771	*SPOCK1*	Sparc/osteonectin, cwcv and kazal-like domains proteoglycan (testican) 1	-2.718465	3	1.112207
11113	*LIG3*	Ligase III, DNA, ATP-dependent	-1.013958	2	0.833472
9448	*MLEC*	Malectin	-1.05939	1	0.817763
1017	*NETO2*	Neuropilin (NRP) and tolloid (TLL)-like 2	-1.639355	2	0.808991
51400	*HIST1H3B*	Histone cluster 1, H3b	-1.070237	1	0.803539
22877	*PHF12*	PHD finger protein 12	-1.531983	1	0.779377
4615	*NCALD*	Neurocalcin δ	-1.345623	2	0.772963
6695	*SIM2*	Single-minded family bHLH transcription factor 2	-2.060616	1	0.707018
79071	*TAB3*	TGF-β activated kinase 1/MAP3K7 binding protein 3	-1.341698	1	0.642641
8358	*MAP4K4*	Mitogen-activated protein kinase kinase kinase kinase 4	-1.043328	1	0.580977
10186	*HNRNPAB*	Heterogeneous nuclear ribonucleoprotein A/B	-1.501292	1	0.571322
11113	*FARP1*	FERM, RhoGEF (ARHGEF) and pleckstrin domain protein 1 (chondrocyte-derived)	-1.379558	1	0.536826
54475	*SPECC1L*	Sperm antigen with calponin homology and coiled-coil domains 1-like	-1.168633	1	0.506925
6548	*NFIB*	Nuclear factor I/B	-1.189804	1	0.505127

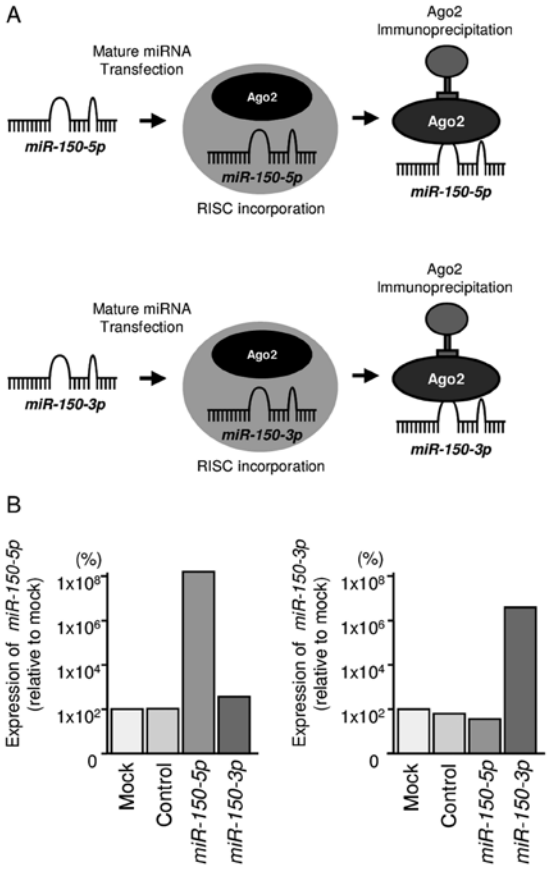

Figure 2. Both *miR-150-5p* and *miR-150-3p* bound to Ago2. (A) Schematic illustration of miRNA detection method. Isolation of RISC incorporated miRNAs by Ago-2 immunoprecipitation. (B) Expression levels of *miR-150-5p* and *miR-150-3p* after transfection with *miR-150-3p* following immunoprecipitation by Ago2 (P<0.0001).

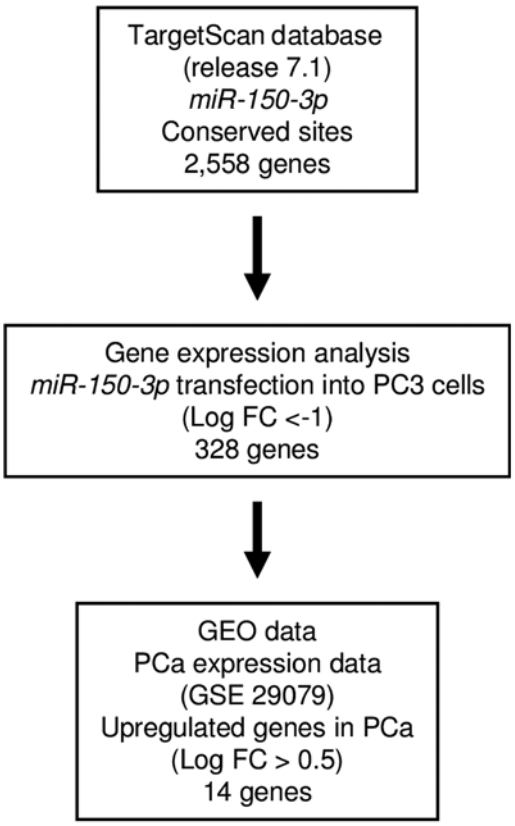

Figure 3. The strategy for analysis of *miR-150-3p* target genes in PCa cells. A total of 2,558 genes were annotated as *miR-150-3p* putative target genes in the TargetScan database (release 7.1). Next, we merged the data for gene expression analysis data in *miR-150-3p* transfectants, and we analyzed gene expression with the available GEO data set (GSE29079). The analyses showed that 14 genes were putative targets of *miR-150-3p* regulation in PCa cells.

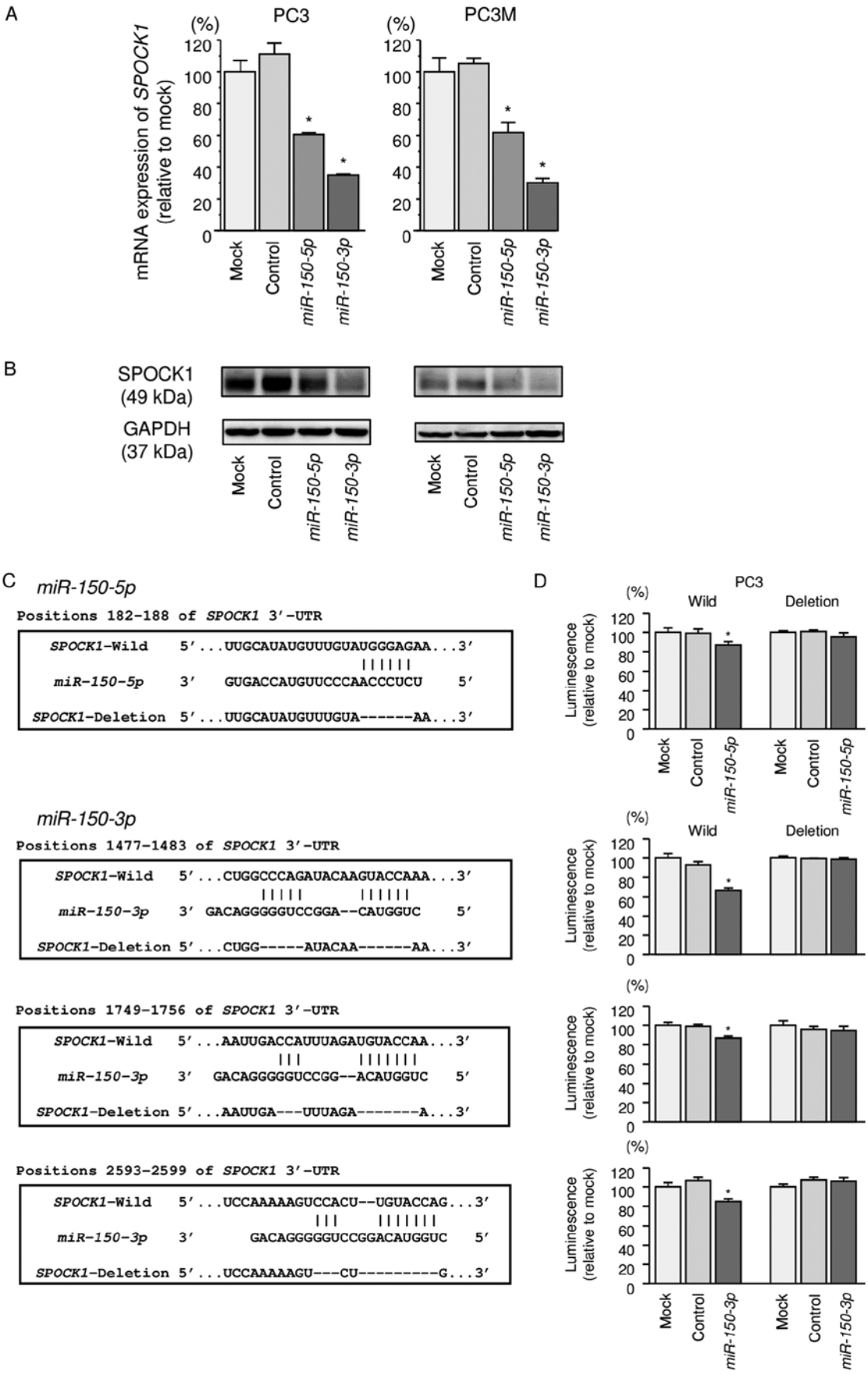

Figure 4. Direct regulation of *SPOCK1* by *miR-150-5p* and *miR-150-3p* in PCa cell lines. (A) *SPOCK1* mRNA expression in PCa cell lines was evaluated by qRT-PCR 72 h after transfection with 10 nM *miR-150-5p* and *miR-150-3p*. GUSB was used as an internal control. *P<0.0001. (B) SPOCK1 protein expression in PCa cell lines was evaluated by western blot analyses 72 h after transfection with *miR-150-5p* and *miR-150-3p*. GAPDH was used as a loading control. (C) *miR-150-5p* or *miR-150-3p* binding sites in the 3'-UTR of *SPOCK1* mRNA. (D) Dual-luciferase reporter assays using vectors encoding putative *miR-150-5p* and *miR-150-3p* target sites of the *SPOCK1* 3'-UTR (positions 182-188, 1477-1483, 1749-1756, and 2593-2599) for both wild-type and deleted regions. Normalized data were calculated as ratios of *Renilla*/firefly luciferase activities. *P<0.05.

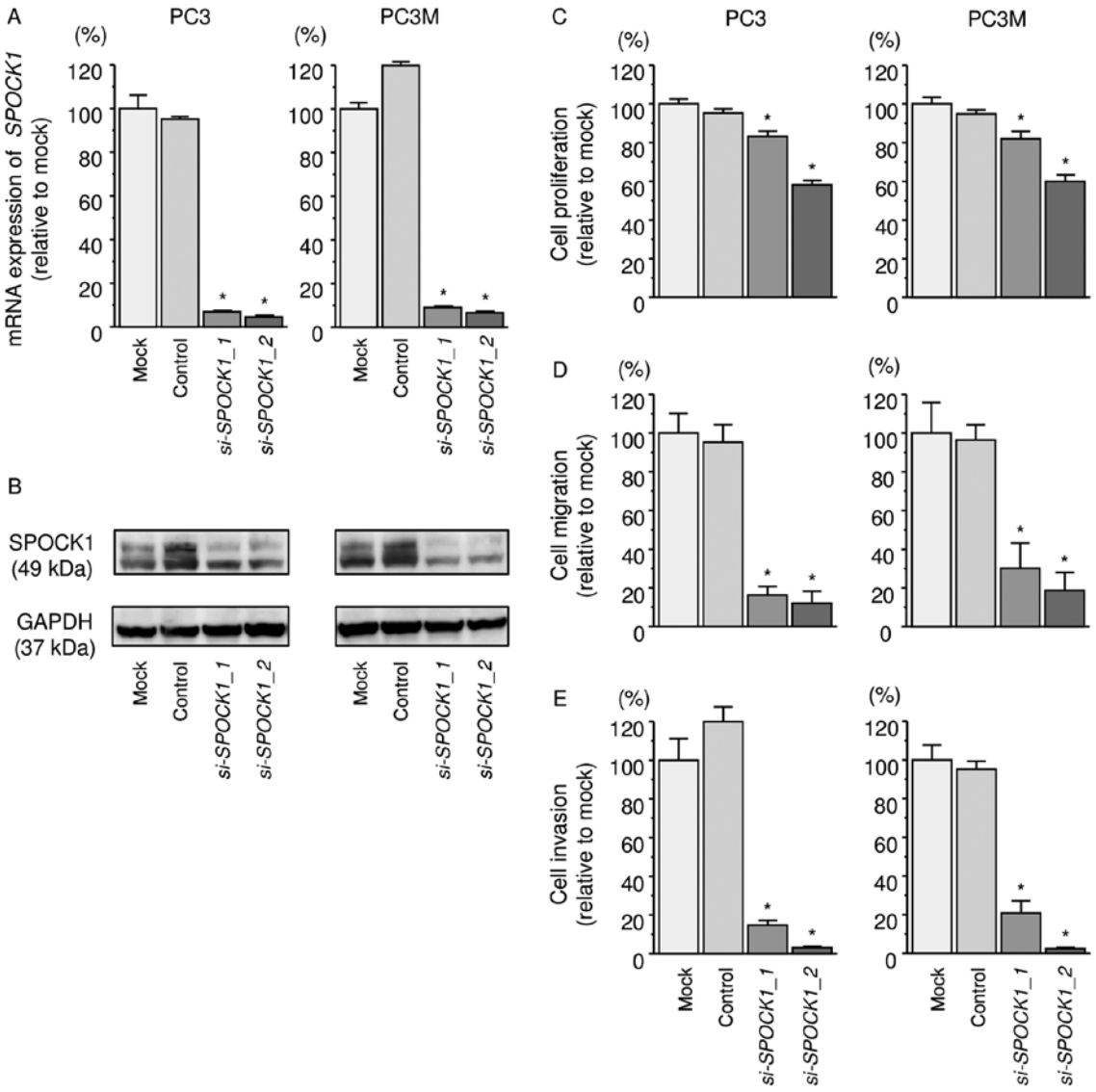

Figure 5. *SPOCK1* mRNA and SPOCK1 protein expression after si-*SPCOK1* transfection and the effects of *SPOCK1* silencing in PCa cell lines. (A) *SPOCK1* mRNA expression in PCa cell lines was evaluated by qRT-PCR 72 h after transfection with 10 nM si-*SPOCK1*_1 or si-*SPOCK1*_2. *GAPDH* was used as an internal control. (B) SPOCK1 protein expression in PCa cell lines was evaluated by western blot analysis 72 h after transfection with siRNAs. GAPDH was used as a loading control. (C) Cell proliferation was determined using XTT assays 72 h after transfection with si-*SPOCK1*_1 or si-*SPOCK1*_2. *P<0.0001. (D) Cell migration activity was determined by migration assays. *P<0.0001. (E) Cell invasion activity was determined using Matrigel invasion assays. *P<0.0001.

tants compared with those in mock- or miR control-transfected cells (P<0.0001, Fig. 5C-E).

Analysis of SPOCK1 expression in naïve PCa and CRPC clinical specimens by immunohistochemistry. Next, we examined the expression levels of SPOCK1 in naïve PCa specimens by immunohistochemical staining. SPOCK1 was strongly expressed in several cancer tissues, while low expression was observed in normal tissues (Fig. 6A). Moreover, the expression score for SPOCK1 protein was significantly higher in PCa tissues than in normal tissues (P<0.001, Fig. 6B). The patient backgrounds and clinicopathological characteristics are summarized in Table II.

To analyze SPOCK1 protein expression, immunohistochemistry was performed with CRPC specimens. Immunohistochemical staining demonstrated high expression of SPOCK1 in CRPC tissues. SPOCK1 was strongly expressed in the cytoplasm of the PCa cells almost in the same area where PSA was expressed (Fig. 6C).

Discussion

Androgen-dependent PCa initially responds to ADT, which can result in disease control. However, most PCa cells eventually acquire ADT-resistance mechanisms. Moreover, there are no curative treatments for patients with metastatic CRPC (19). One of the main challenges in treating CRPC is controlling aggressive, lethal metastatic PCa cells. We believe identification of the genes and pathways responsible for metastasis may lead to the development of new therapeutic strategies. Accordingly, we have focused on identifying antitumor miRNAs and oncogenic RNA networks mediated by these miRNAs in naïve PCa and CRPC cells (9,20,21). For example, antitumor miR-223 inhibits cancer cell migration and invasion by targeting *ITGA3*

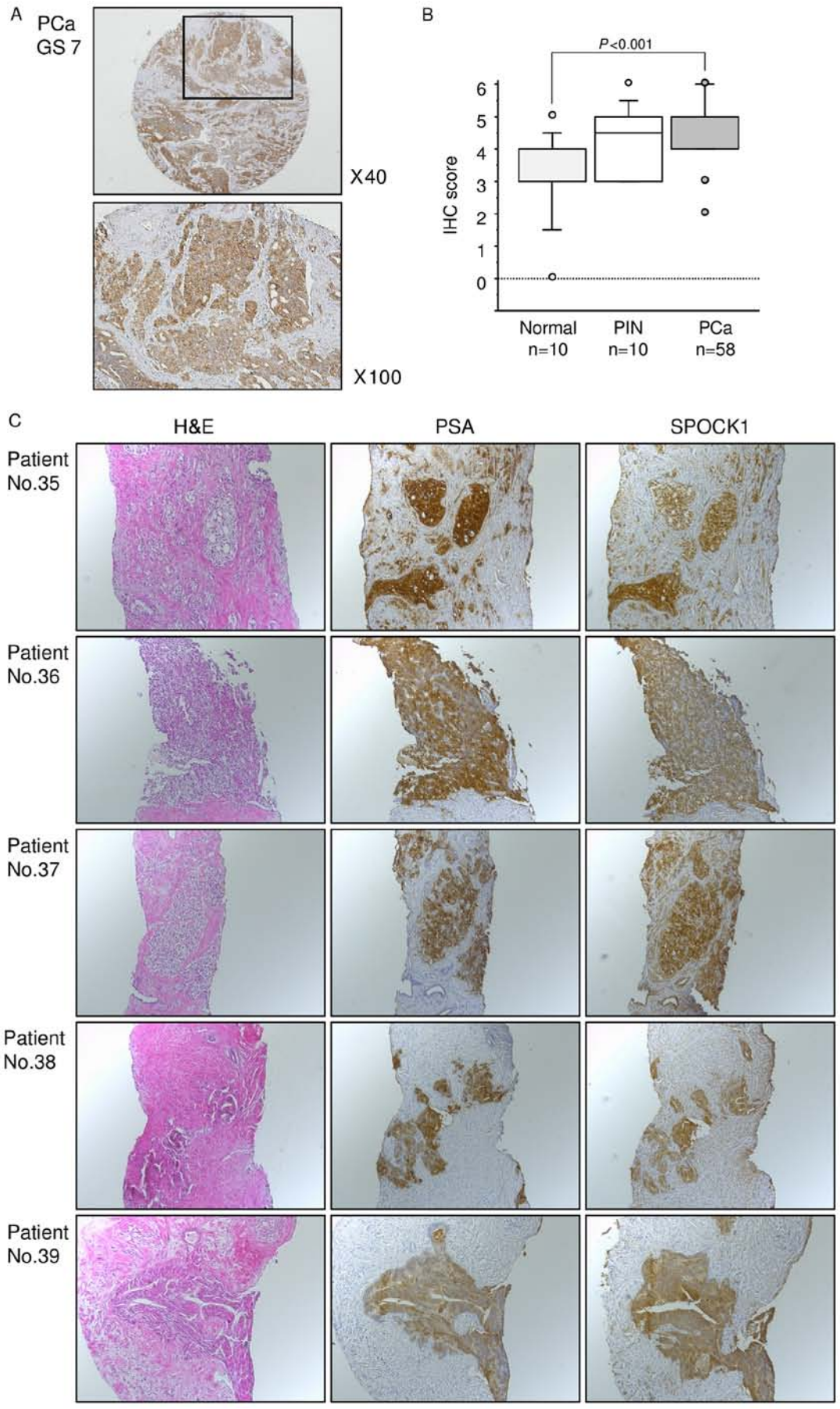

Figure 6. Immunohistochemical staining of SPOCK1 protein in naïve PCa and CRPC specimens. (A) Immunohistochemical staining of SPOCK1 in naïve PCa using a tissue microarray. SPOCK1 was strongly expressed in several cancer tissues, while low expression was observed in normal tissues. (B) Quantification of SPOCK1 expression in PCa (n=58), PIN (n=10), and normal prostatic tissue (n=10) by tissue microarray. (C) Expression of SPOCK1 in CRPC specimens. SPOCK1 was strongly expressed in cancer lesions, similar to PSA.

and *ITGB1* (18). Antitumor *miR-218* suppresses migration and invasion by regulating *LASP1* (22). Moreover, antitumor miRNAs (*miR-26a/b, miR-29a/b/c* and *miR-218*) function cooperatively to suppress metastasis-promoting *LOXL* (23).

In this study, we demonstrated that the dual strands of pre-*miR-150*, i.e., *miR-150-5p* and *miR-150-3p*, acted as antitumor miRNAs in naïve PCa and CRPC cells. According to the miRNA database (miRBase: http://www.mirbase.org/), *miR-150-5p* is a guide strand of pre-*miR-150*, and *miR-150-3p* is the corresponding passenger strand. Previous studies have shown that *miR-150-5p* (the guide strand) is frequently downregulated in cancer tissues and functions as an antitumor miRNA in several types of cancer (24-26). In this study, we focused on *miR-150-3p* (the passenger strand) and investigated the antitumor roles of this miRNA in naïve PCa and CRPC cells because no prior studies had evaluated the functions of *miR-150-3p* in cancer cells.

Passenger strands of miRNA are thought to be degraded and are not expected to be incorporated into the RISC (4). However, our data showed that the passenger strand of *miR-150* was incorporated into the RISC in PCa cells, and this is the first report of the antitumor function of *miR-150-3p* in cancer cells. Our recent studies demonstrated that *miR-145-3p* (the passenger strand of pre-*miR-145*) acted as an antitumor miRNA targeting oncogenic *UHRF1* and *MTDH* in bladder and lung cancer, respectively (16,27). Similarly, we confirmed the antitumor function of *miR-139-3p* (a passenger strand of pre-*miR-139*) in bladder cancer (17). These findings suggested that the passenger strands of miRNAs may have some biological functions in human cells, similar to the guide strands of miRNAs. The involvement of passenger strand miRNAs in the regulation of cellular processes is a novel concept in RNA research.

One of the main challenges in miRNA studies is to seek out miRNA targeting genes and RNA networks mediated by these miRNAs in cancer cells. We revealed that *SPOCK1* was a direct target of dual strands of *miR-150-5p* and *miR-150-3p* in PCa cells. Moreover, we demonstrated the overexpression of SPOCK1 in naïve PCa and CRPC clinical specimens. *SPOCK1/testican-1* belongs to the Ca^{2+}-binding proteoglycan family, which includes SPARC, testican-2, and testican-3 (28). Overexpression of *SPOCK1* was observed in several cancers and has been shown to play pivotal roles in cancer cell progression, metastasis, and drug resistance (29-31). *SPOCK1* is upregulated in lung cancer and is associated with metastasis and survival (32). Interestingly, ectopic expression of *SPOCK1* induces the epithelial-mesenchymal transition (EMT) in lung cancer cells (33). Another study demonstrated that *SPOCK1* induces MET-dependent EMT signaling in lapatinib-resistant gastric cancer (34). Several reports have indicated that tyrosine kinase receptor inhibitors (TKIs) can frequently cause the acquisition of TKI resistance in cells and that the EMT is deeply involved in these events (35,36). These findings suggest that *SPOCK1* mediates the EMT signaling to regulate cancer cell aggressiveness and drug resistance.

Most patients with PCa exhibit ADT failure and progress to CRPC with metastasis. Moreover, no curative treatments are available for advanced CRPC with metastasis (37). In CRPC cells, the EMT is associated with metastatic processes and is involved in drug resistance (38). Interestingly, androgens and androgen receptor-mediated signaling enhance the EMT and cancer cell aggressiveness (39). Transforming growth factor β (TGFβ) is a pivotal player that induces EMT in cancer cells (40). Increased expression of TGFβ and EMT-related proteins has been observed in CRPC bone metastasis (41). Interestingly, expression of SPOCK1 is elevated by TGFβ treatment in lung cancer cells, suggesting that *SPOCK1* mediates downstream TGFβ signaling (33). We suggest that *SPOCK1* expression may be related to induction of TGFβ signaling and epigenetic regulation of *miR-150-5p* and *miR-150-3p* in naïve PCa and CRPC cells. A recent study showed that overexpression of *SPOCK1* in RWPE-1 cells (non-neoplastic adult human prostatic epithelial cells) promotes cell viability and cell migration and invasion abilities (42). These findings were supported by our present data. Thus, the expression of *SPOCK1* may be involved in the pathogenesis of naïve PCa and CRPC, and *SPOCK1*-mediated signaling may be a promising therapeutic target in this disease.

In conclusiom, the dual strands of pre-miR-150, i.e., *miR-150-5p* and *miR-150-3p*, were significantly reduced in naïve PCa and CRPC tissues and acted as antitumor mRNAs. The passenger strand of *miR-150-3p* was found to have a specific function in cancer cells. *SPOCK1* was directly regulated by dual strands of *miR-150-5p* and *miR-150-3p* in PCa cells. Overexpression of *SPOCK1* was confirmed in naïve PCa and CRPC tissues and acted as an oncogene in this disease. Elucidation of *miR-150/SPOCK1*-mediated molecular networks may lead to a better understanding of the pathogenesis of naïve PCa and CRPC and facilitate the development of new treatment strategies.

Acknowledgements

This study was supported by KAKENHI grants 15K10801(C), 15K20071(C), 16K20125, and 16H05462(B).

References

1. Siegel RL, Miller KD and Jemal A: Cancer Statistics, 2017. CA Cancer J Clin 67: 7-30, 2017.
2. Sridhar SS, Freedland SJ, Gleave ME, Higano C, Mulders P, Parker C, Sartor O and Saad F: Castration-resistant prostate cancer: From new pathophysiology to new treatment. Eur Urol 65: 289-299, 2014.
3. Sturge J, Caley MP and Waxman J: Bone metastasis in prostate cancer: Emerging therapeutic strategies. Nat Rev Clin Oncol 8: 357-368, 2011.
4. Bartel DP: MicroRNAs: Genomics, biogenesis, mechanism, and function. Cell 116: 281-297, 2004.
5. Carthew RW and Sontheimer EJ: Origins and mechanisms of miRNAs and siRNAs. Cell 136: 642-655, 2009.
6. Zhang Y, Wang Z and Gemeinhart RA: Progress in microRNA delivery. J Control Release 172: 962-974, 2013.
7. Bartel DP: MicroRNAs: Target recognition and regulatory functions. Cell 136: 215-233, 2009.
8. Nelson KM and Weiss GJ: MicroRNAs and cancer: Past, present, and potential future. Mol Cancer Ther 7: 3655-3660, 2008.
9. Goto Y, Kojima S, Nishikawa R, Kurozumi A, Kato M, Enokida H, Matsushita R, Yamazaki K, Ishida Y, Nakagawa M, *et al*: MicroRNA expression signature of castration-resistant prostate cancer: The microRNA-221/222 cluster functions as a tumour suppressor and disease progression marker. Br J Cancer 113: 1055-1065, 2015.
10. Okato A, Goto Y, Kurozumi A, Kato M, Kojima S, Matsushita R, Yonemori M, Miyamoto K, Ichikawa T and Seki N: Direct regulation of LAMP1 by tumor-suppressive microRNA-320a in prostate cancer. Int J Oncol 49: 111-122, 2016.

11. Gregory RI, Chendrimada TP, Cooch N and Shiekhattar R: Human RISC couples microRNA biogenesis and posttranscriptional gene silencing. Cell 123: 631-640, 2005.
12. Chendrimada TP, Gregory RI, Kumaraswamy E, Norman J, Cooch N, Nishikura K and Shiekhattar R: TRBP recruits the Dicer complex to Ago2 for microRNA processing and gene silencing. Nature 436: 740-744, 2005.
13. Hutvágner G and Zamore PD: A microRNA in a multiple-turnover RNAi enzyme complex. Science 297: 2056-2060, 2002.
14. Matranga C, Tomari Y, Shin C, Bartel DP and Zamore PD: Passenger-strand cleavage facilitates assembly of siRNA into Ago2-containing RNAi enzyme complexes. Cell 123: 607-620, 2005.
15. Sobin LH, Gospodarowicz MK and Wittekind Ch (eds.): TNM Classification of Malignant Tumours. 7th edition. Wiley-Blackwell, Chichester, 2009.
16. Mataki H, Seki N, Mizuno K, Nohata N, Kamikawaji K, Kumamoto T, Koshizuka K, Goto Y and Inoue H: Dual-strand tumor-suppressor microRNA-145 (miR-145-5p and miR-145-3p) coordinately targeted MTDH in lung squamous cell carcinoma. Oncotarget 7: 72084-72098, 2016.
17. Yonemori M, Seki N, Yoshino H, Matsushita R, Miyamoto K, Nakagawa M and Enokida H: Dual tumor-suppressors miR-139-5p and miR-139-3p targeting matrix metalloprotease 11 in bladder cancer. Cancer Sci 107: 1233-1242, 2016.
18. Kurozumi A, Goto Y, Matsushita R, Fukumoto I, Kato M, Nishikawa R, Sakamoto S, Enokida H, Nakagawa M, Ichikawa T, *et al*: Tumor-suppressive microRNA-223 inhibits cancer cell migration and invasion by targeting ITGA3/ITGB1 signaling in prostate cancer. Cancer Sci 107: 84-94, 2016.
19. Semenas J, Allegrucci C, Boorjian SA, Mongan NP and Persson JL: Overcoming drug resistance and treating advanced prostate cancer. Curr Drug Targets 13: 1308-1323, 2012.
20. Fuse M, Kojima S, Enokida H, Chiyomaru T, Yoshino H, Nohata N, Kinoshita T, Sakamoto S, Naya Y, Nakagawa M, *et al*: Tumor suppressive microRNAs (miR-222 and miR-31) regulate molecular pathways based on microRNA expression signature in prostate cancer. J Hum Genet 57: 691-699, 2012.
21. Goto Y, Kurozumi A, Enokida H, Ichikawa T and Seki N: Functional significance of aberrantly expressed microRNAs in prostate cancer. Int J Urol 22: 242-252, 2015.
22. Nishikawa R, Goto Y, Sakamoto S, Chiyomaru T, Enokida H, Kojima S, Kinoshita T, Yamamoto N, Nakagawa M, Naya Y, *et al*: Tumor-suppressive microRNA-218 inhibits cancer cell migration and invasion via targeting of LASP1 in prostate cancer. Cancer Sci 105: 802-811, 2014.
23. Kato M, Kurozumi A, Goto Y, Matsushita R, Okato A, Nishikawa R, Fukumoto I, Koshizuka K, Ichikawa T and Seki N: Regulation of metastasis-promoting LOXL2 gene expression by antitumor microRNAs in prostate cancer. J Hum Genet 62: 123-132, 2017.
24. Abe F, Kitadate A, Ikeda S, Yamashita J, Nakanishi H, Takahashi N, Asaka C, Teshima K, Miyagaki T, Sugaya M, *et al*: Histone deacetylase inhibitors inhibit metastasis by restoring a tumor suppressive microRNA-150 in advanced cutaneous T-cell lymphoma. Oncotarget 8: 7572-7585, 2017.
25. Srivastava SK, Bhardwaj A, Singh S, Arora S, Wang B, Grizzle WE and Singh AP: MicroRNA-150 directly targets MUC4 and suppresses growth and malignant behavior of pancreatic cancer cells. Carcinogenesis 32: 1832-1839, 2011.
26. Qu Y, Pan S, Kang M, Dong R and Zhao J: MicroRNA-150 functions as a tumor suppressor in osteosarcoma by targeting IGF2BP1. Tumour Biol 37: 5275-5284, 2016.
27. Matsushita R, Yoshino H, Enokida H, Goto Y, Miyamoto K, Yonemori M, Inoguchi S, Nakagawa M and Seki N: Regulation of UHRF1 by dual-strand tumor-suppressor microRNA-145 (miR-145-5p and miR-145-3p): Inhibition of bladder cancer cell aggressiveness. Oncotarget 7: 28460-28487, 2016.
28. Bradshaw AD: Diverse biological functions of the SPARC family of proteins. Int J Biochem Cell Biol 44: 480-488, 2012.
29. Li Y, Chen L, Chan TH, Liu M, Kong KL, Qiu JL, Li Y, Yuan YF and Guan XY: SPOCK1 is regulated by CHD1L and blocks apoptosis and promotes HCC cell invasiveness and metastasis in mice. Gastroenterology 144: 179-191.e4, 2013.
30. Ma LJ, Wu WJ, Wang YH, Wu TF, Liang PI, Chang IW, He HL and Li CF: SPOCK1 Overexpression confers a poor prognosis in urothelial carcinoma. J Cancer 7: 467-476, 2016.
31. Shu YJ, Weng H, Ye YY, Hu YP, Bao RF, Cao Y, Wang XA, Zhang F, Xiang SS, Li HF, *et al*: SPOCK1 as a potential cancer prognostic marker promotes the proliferation and metastasis of gallbladder cancer cells by activating the PI3K/AKT pathway. Mol Cancer 14: 12, 2015.
32. Kusakabe M, Kutomi T, Watanabe K, Emoto N, Aki N, Kage H, Hamano E, Kitagawa H, Nagase T, Sano A, *et al*: Identification of G0S2 as a gene frequently methylated in squamous lung cancer by combination of in silico and experimental approaches. Int J Cancer 126: 1895-1902, 2010.
33. Miao L, Wang Y, Xia H, Yao C, Cai H and Song Y: SPOCK1 is a novel transforming growth factor-β target gene that regulates lung cancer cell epithelial-mesenchymal transition. Biochem Biophys Res Commun 440: 792-797, 2013.
34. Kim HP, Han SW, Song SH, Jeong EG, Lee MY, Hwang D, Im SA, Bang YJ and Kim TY: Testican-1-mediated epithelial-mesenchymal transition signaling confers acquired resistance to lapatinib in HER2-positive gastric cancer. Oncogene 33: 3334-3341, 2014.
35. Uramoto H, Iwata T, Onitsuka T, Shimokawa H, Hanagiri T and Oyama T: Epithelial-mesenchymal transition in EGFR-TKI acquired resistant lung adenocarcinoma. Anticancer Res 30: 2513-2517, 2010.
36. Choe C, Shin YS, Kim C, Choi SJ, Lee J, Kim SY, Cho YB and Kim J: Crosstalk with cancer-associated fibroblasts induces resistance of non-small cell lung cancer cells to epidermal growth factor receptor tyrosine kinase inhibition. Onco Targets Ther 8: 3665-3678, 2015.
37. Crawford ED, Higano CS, Shore ND, Hussain M and Petrylak DP: Treating patients with metastatic castration resistant prostate xancer: A comprehensive review of available therapies. J Urol 194: 1537-1547, 2015.
38. Martin SK, Pu H, Penticuff JC, Cao Z, Horbinski C and Kyprianou N: Multinucleation and mesenchymal-to-epithelial transition alleviate resistance to combined cabazitaxel and anti-androgen therapy in advanced prostate cancer. Cancer Res 76: 912-926, 2016.
39. Nakazawa M and Kyprianou N: Epithelial-mesenchymal-transition regulators in prostate cancer: Androgens and beyond. J Steroid Biochem Mol Biol 166: 84-90, 2017.
40. Xu J, Lamouille S and Derynck R: TGF-beta-induced epithelial to mesenchymal transition. Cell Res 19: 156-172, 2009.
41. Haider M, Zhang X, Coleman I, Ericson N, True LD, Lam HM, Brown LG, Ketchanji M, Nghiem B, Lakely B, *et al*: Epithelial mesenchymal-like transition occurs in a subset of cells in castration resistant prostate cancer bone metastases. Clin Exp Metastasis 33: 239-248, 2016.
42. Chen Q, Yao YT, Xu H, Chen YB, Gu M, Cai ZK and Wang Z: SPOCK1 promotes tumor growth and metastasis in human prostate cancer. Drug Des Devel Ther 10: 2311-2321, 2016.